XI International Conference on Computational Plasticity. Fundamentals and Applications
COMPLAS XI
E. Oñate, D.R.J. Owen, D. Peric and B. Suárez (Eds)

A MICROMECHANICAL CONSTITUTIVE MODEL FOR DUCTILE FRACTURE: NUMERICAL TREATMENT AND CALIBRATION STRATEGY

L. Malcher *, F.M. Andrade Pires†, J.M.A. César de Sá†

* Automotive Engineering Area, Faculty UnB Gama, University of Brasilia,
Distrito Federal, Brazil
e-mail: malcher@unb.br

† Department of Mechanical Engineering, Faculty of Engineering, University of Porto
Rua Dr. Roberto Frias, Porto 4200-465, Portugal

Key words: Micromechanical Model, Ductile Fracture, Two Damage Parameters.

Abstract. This contribution describes the numerical treatment and calibration strategy for a new micromechanical damage model, which employs two internal damage variables. The new micromechanical model is based on Gurson's theory incorporating the void volume fraction as one damage parameter and a shear mechanism, which was formulated considering geometrical and phenomenological aspects, as the second internal damage variable. The first and the second damage variables are coupled in the constitutive formulation in order to affect the hydrostatic stress and deviatoric stress contributions, respectively. Both internal damage variables are independent and, as a consequence, they also require independent nucleation mechanisms for each one in order to trigger the growth contribution. These mechanisms require the determination of material parameters that are obtained through two calibration points: one for high and the other for low stress triaxiality. This is in contrast to other damage models that typically require one calibration point. In the first part of this paper, theoretical aspects of the constitutive formulation are presented and discussed. Then, an implicit numerical integration algorithm is derived, based on the operator split methodology, together with a methodology to perform the calibration of all material parameters. In order to assess the performance of the new model, the "butterfly" specimen was used and the 1045 steel was employed under a wide range of stress triaxiality. The results obtained from the numerical simulations are presented such as: the evolution of both damage parameters, the evolution of the equivalent plastic strain, the reaction versus displacement curve and the contour of the effective damage parameter. From the comparison of the numerical results with experimental evidence, it will be highlighted that the present formulation is able to predict accurately the location of fracture onset and the level of the associated equivalent plastic strain at fracture.

1 INTRODUCTION

Ductile fracture in metals is an important subject to be improved in order to predict the correct location of crack initiation in machine components and rupture in general structures. The fracture phenomenon can be studied by its separated evolution contribution as the initiation and growth of general micro defects which is induced by large deformations. Some

researchers like McClintock [15] and Rice & Tracey [21] developed pioneering work undertaken on the subject, where the nature of defect was taken into account the study of ductile damage by analyzing its geometry in a continuous matrix.

The degradation of material properties is an irreversible process and starts from the formation of micro defects which can be voids, cracks and others, that already exist or that will be formed in the material matrix. However, the evolution of material degradation is dependent on macroscopic loading conditions which can cause a volumetric void growth such as in tensile loading condition or a preferential elongation of micro defects which can be observed in pure shear loading conditions. The ductile fracture phenomenon can be described, based on a micromechanical analysis of micro cavity growth, especially for the fracture computation within local approaches of fracture, (see Pineau [19]; Mudry [16]; Rousselier [23]; Besson [3]) or based on the Continuum Damage Mechanics theory and a thermodynamic framework, either phenomenological or micromechanically based, as Lemaitre [12].

The formulations proposed by Lemaitre and Gurson are the most important coupled damage ductile models to describe the above two methodologies, see Chaboche [7]. Since then, motivated by the limitations of these classical models, such as in prediction of the correct fracture location or in determination of the correct values of the internal variables at fracture, many researchers have proposed improvements in both methodologies, by introducing more effects in the constitutive formulation or in the damage evolution law like the pressure effect, temperature, Lode angle dependence, viscoplastic effects, crack closure effect, shear mechanisms, among others (Tvergaard & Needleman [27]; Rousselier [22;24]; Xue [28]; Nahshon & Hutchinson [17]; Lemaitre & Chaboche [13]; Chaboche [6]; Andrade Pires [1]; Chaboche et al. [7] ; Besson [4]).

These classical coupled damage models have the ability to predict the correct fracture location under a specific range of stress triaxialities (see Xue [28]; Nahshon [17]; Teng [26]) and are extremely accurate for loading conditions close to the calibration point, see Malcher [14]. For example, within range of high levels of stress triaxialities, where the spherical void growth is the predominant mechanism, the models based on Gurson theory, like the Gurson-Tvergaard-Needleman model, have good performance in prediction of fracture location and parameters in fracture as equivalent plastic strain and displacement. However, under shear dominated loads, where failure is mainly driven by the shear localization of plastic strain of the inter-voids ligaments due to void rotation and distortion, the model does not perform well, see Engelen [9] and Chaboche [7].

Due to these two types of ductile failure mechanisms, it is expected that the population of micro defects, that can be nucleated, would be higher in void sheeting than in internal necking. Motivated by these short comings, in this contribution, a new extension to the GTN model is proposed in order to improve the ability to predict the correct fracture location and determinate the internal parameters in the fracture. A new independent damage parameter is suggested to capture elongation of micro-defects and coupled to constitutive model to affect only the deviatoric stress part. A nucleation of general micro defects is introduced to trigger the shear mechanism and gives more accuracy to the model in prediction of ductile failure under mixed loading condition.

2 CONTITUTIVE FORMULATION

One of the most popular versions of Gurson's model is the Tvergaard–Needleman modification (Tvergaard and Needleman [27]). The model assumes isotropic hardening and isotropic damage, represented by the effective porosity f^*. The constitutive formulation for GTN's model can be better expressed as:

$$\Phi(\boldsymbol{\sigma}, k, f) = J_2(\boldsymbol{S}) - \frac{1}{3}\left\{1 + q_3.f^{*2} - 2.q_1.f^*.\cosh\left(\frac{q_2.3.p}{2.\sigma_y}\right)\right\}.\sigma_y{}^2 \tag{1}$$

where, the parameters q_1, q_2 and q_3 are introduced to bring the model predictions into closer agreement with full numerical analyses of a periodic array of voids.

The damage evolution, in this formulation, is reproduced by three simultaneous or successive mechanisms that can be described as the nucleation, growth and coalescence of voids as

$$f^* = \begin{cases} f, & f < f_c \\ f_c + \left(\frac{1}{q_1} - f_c\right)\frac{(f - f_c)}{(f_f - f_c)}, & f \geq f_c \end{cases} \tag{2}$$

where, f^* represents the effective damage, f_c denotes the critical volume void fraction and f_f is the volume void fraction at fracture. The effective damage is determined based on both nucleation and growth mechanisms if the volume void fraction is less than critical value. The coalescence is active only if the volume void fraction is higher than the critical value. The volume void fraction rate, $\dot{f}$, is a sum of the nucleation and growth mechanism as.

$$\dot{f} = \dot{f}^n + \dot{f}^g \tag{3}$$

The nucleation mechanism can be driven by either the plastic strain or the hydrostatic pressure. Equation 4 represents the nucleation mechanism based on the equivalent plastic strain:

$$\dot{f}^n = \frac{f_N}{s_N.\sqrt{2\pi}}.\exp\left[-\frac{1}{2}\left(\frac{\bar{\varepsilon}^p - \varepsilon_N}{s_N}\right)^2\right]\dot{\bar{\varepsilon}}^p \tag{4}$$

where, f_N represents the volume fraction of all second-phase particles with potential for microvoid nucleation, ε_N and s_N are the mean strain/pressure for void nucleation and its standard deviation. The variable $\bar{\varepsilon}^p$ represents the equivalent plastic strain and $\dot{\bar{\varepsilon}}^p$ is the rate of the accumulated plastic strain. The nucleation mechanism is valid only if the hydrostatic pressure is great to zero, $p > 0$. If $p \leq 0$, the nucleation mechanism rate is equal to zero. The evolution of growth mechanism in GTN's model is determined as:

$$\dot{f} = (1 - f).\dot{\varepsilon}_v^p \tag{5}$$

where, the elastic strain rate contributions is represented by $\dot{\varepsilon}_v^e$.

In order to improve the micromechanical models like Gurson and GTN to predict failure when void sheeting mechanism plays the main role, researchers as Xue [28], Nahshon & Hutchinson [17], Butcher et al. [5] have suggested the introduction of another mechanism as

shear, in the evolution law of the Gurson's damage parameter. Both researchers have initially formulated shear mechanisms based on phenomenological and geometrical aspects resulting in expression dependent on the equivalent plastic strain and its rate and a Lode angle function. Both formulations have shown a very nice performance in pure loading conditions, regarding the prediction of the crack initiation, but in combined load path, the models have failed either in prediction of the fracture location or in level of equivalent strain and displacement at fracture, see Malcher [14] and Reis & Malcher [20]). Xue [28], based on volume conservation of a representative square cell contains a cylindrical void at the center, has proposed a shear mechanism when this cell structure is subjected a pure shear loading condition. The evolution law for the shear mechanism proposed by Xue is represented by Equation 6

$$\dot{D}_{shear} = q_4 f^{q_5} \varepsilon_{eq} . \dot{\varepsilon}_{eq} \tag{6}$$

where, q_4 and q_5 are geometrical parameters and can be defined according to two or three dimensional problem. For two dimensional problem, $q_4 = \frac{3}{\sqrt{\pi}}$ and $q_5 = (1/2)$ and for three dimensional problem, $q_4 = \frac{3}{2}\left(\frac{6}{\pi}\right)^{(1/3)}$ and $q_5 = (1/3)$.

The shear mechanisms can be coupled in GTN's model and a so called Lode angle function is required to active the mechanism only when the shear strain is detected in a general loading condition. Xue [28] defines the Lode angle function as a linear expression of the normalized Lode angle, as:

$$g_0 = (1 - |\bar{\theta}|) \tag{7}$$

where, g_0 represents the so called Lode angle function and $\bar{\theta}$ is the normalized Lode angle. Thus, the damage internal variable rate (Equation 3) can be re-written according Equation 8.

$$\dot{f} = \dot{f}^n + \dot{f}^g + \dot{D}_{shear} \tag{8}$$

Authors as Reis & Malcher [20], Malcher [14], Xue [28] and Nahshon & Hutchinson [17] have shown that the original GTN's model has limitations, such as: no ability to predict failure in pure shear loading condition, due to the fact that the growth rate of the volume void fraction, which plays the damage parameter role, has no evolution; the coupled damage models have got good performance only for loading conditions close to calibration point; the nucleation of micro-voids mechanism does not have a physical meaning in low stress triaxiality, since the nucleation of micro-defects, in general, can be better appointed; and, in the plastic flow rule, the deviatoric stress tensor contribution is not affected by the damage parameter and the volume void fraction affects only the hydrostatic stress term. However, in order to try to solve the above problems, in this paper, a new formulation for GTN original model is suggested, giving ability to predict the correct location to crack initiation and the determination of the values of the internal variables at fracture.

The proposition starts from the way that the shear damage parameter is coupled in the GTN yield function. In the GTN original model (see Tvergaard and Needleman [27]) or in the GTN improved model (see Xue [28]; Nahshon & Hutchinson [17]), the damage parameters, such as only porosity or porosity and shear damage, affect mainly the hydrostatic pressure

contribution (see Equation 1). Hence, in this case, the plastic flow rule is expressed by an unbalanced equation, which the deviatoric contribution is free of the damage parameters. In this contribution, the volume void fraction and the shear damage will be coupled disconnectedly in the yield surface. The volume void fraction will affect exclusively the hydrostatic pressure and the shear damage will be coupled affecting the deviatoric stress contribution. Thus, Equation 1 can be re-written as follow:

$$\Phi(\boldsymbol{\sigma}, k, f) = \frac{J_2(\boldsymbol{S})}{(1 - D^{shear})} - \frac{1}{3}\left\{1 + q_3.f^2 - 2.q_1.f.\cosh\left(\frac{q_2.3.p}{2.\sigma_y}\right)\right\}.\sigma_y{}^2 \tag{9}$$

The new yield function would still be a function of the set of parameters $[\boldsymbol{\sigma}, k, f]$, since than the shear mechanism would still be a function of the volume void fraction.

In this paper, it is suggested an uncoupling between both shear damage and volume void fraction as well as the creation of a new nucleation of micro defects mechanism, responsible to trigger the shear damage parameter. Thus, the new constitutive formulation will get two independent damage parameters and the yield function established by Equation 9 would be a function of the set of parameters $[\boldsymbol{\sigma}, k, f, D]$. The volume void fraction, as defined by Tvergaard & Needleman [27] would be the first damage parameter and shear damage with a new nucleation of micro defect mechanism, the second one. Hence, the evolution of the new damage parameter can be expressed as:

$$\dot{D} = \dot{D}^n + q_6.\dot{D}^{shear} \tag{10}$$

where $\dot{D}$ represents the rate of the new damage parameter, $\dot{D}^n$ represents the rate of the nucleation of micro defects mechanism, $\dot{D}^{shear}$ denotes the rate of the shear contribution and the parameter q_6 can be introduced to calibrate the rate of the shear contribution, bringing more flexibility to suit the critical shear damage with the experimental critical displacement.

The nucleation of micro defects mechanisms, by the authors, will be considered a normal distribution of all second-phase particles with potential for micro defect nucleation and can be expressed as:

$$\dot{D}^n = \frac{D_N}{s'_N.\sqrt{2\pi}}.\exp\left[-\frac{1}{2}\left(\frac{\bar{\varepsilon}^p - \varepsilon'_N}{s'_N}\right)^2\right]\dot{\bar{\varepsilon}}^p \tag{11}$$

where, D_N represents the fraction of all second-phase particles with potential for micro defect nucleation, ε'_N and s'_N are the mean strain for defect nucleation and its standard deviation. The set of parameters $[D_N, \varepsilon'_N, s'_N]$, required to the nucleation of micro defect, need to be calibrated for a point in pure shear loading condition. This contribution added a new calibration point further the already required, which can come a very nice accuracy for the formulation within the all range of stress triaxiality.

Regarding the same simplification adopted by Gurson [11], in order to vanish the elastic contribution in the definition of the volume void fraction rate for a rigid plastic matrix (see Equation 5), the authors can suggest that in the rate of the shear mechanisms (Equation 6)

contribution, both equivalent strain and equivalent strain rate would be changed by the equivalent plastic strain and equivalent plastic strain rate. This simplification is reasonable in the majority of problems involving ductile damage since the elastic strains can be considered negligible. Thus, the expressions can be re-written, as:

$$\dot{D}^{shear} = q_4 D^{q_5} \bar{\varepsilon}^p . \dot{\bar{\varepsilon}}^p \tag{12}$$

By the authors and through the experimental evidence, the stress triaxiality effect can be introduced by an exponent in the previous Lode angle functions suggested by Xue.

$$g_0'(\xi,\eta) = [g_0(\xi)]^{1/\|\eta\|+k} \tag{13}$$

where, g_0' is the new function that now will be called by balance function, η represents the stress triaxiality and k is a constant that need to be calibrated. Figure 1 represents the behavior of the balance function on the space of the set of parameters $[g_0, \xi, \eta]$. The influence of the stress triaxiality can be observed manly in the range of stress triaxiality between $[-1/3 ; 1/3]$.

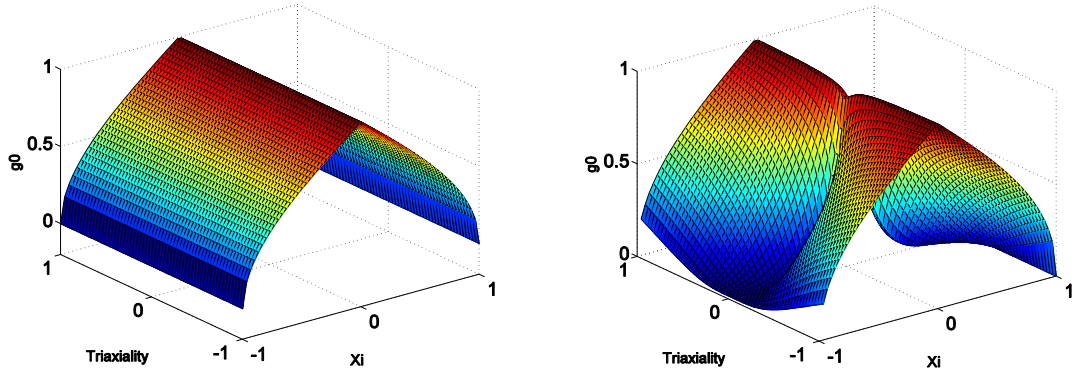

(a) (b)

Figure 1: Three dimensional representation of the balance function suggested by the authors.

Regarding this new model, two independents nucleation mechanisms are introduced, first one to trigger the growth rate of the volume void fraction and the second one to trigger the growth rate of the shear mechanism. In order to active or not each one contribution when pure shear or pure tensile loading condition is applied or to balance the value of it when both shear/tensile or shear/compression loading condition is present, the authors suggest the introduction of the Lode angle function, g_0, in the nucleation mechanisms

How was previously discussed, based on the modified formulation, two calibration points are required. First one for high stress triaxiality, which the smooth bar specimen can be used to determine the hardening law, σ_y, for undamaged model, the void nucleation parameters as f_N, ε_N and S_N and the critical volume void fraction f_c. A specimen in pure shear loading condition is also required to calibrate the general micro defects nucleation parameters as D_N, ε_N^s and s_N^s, the accelerator damage parameter, q_6, and the critical shear damage parameter, D_c. In Box 1, the basic constitutive equations and evolution law for internal variable and damage parameters are summarized:

Box 1. GTN's modified model including nucleation and elongation of micro shear defects.

(i) Elasto-plastic split of the strain tensor:

$$\boldsymbol{\varepsilon} = \boldsymbol{\varepsilon}^{e} + \boldsymbol{\varepsilon}^{p}$$

(ii) Elastic law

$$\boldsymbol{\sigma} = \mathbb{D}^{e} : \boldsymbol{\varepsilon}^{e}$$

(iii) Yield function

$$\Phi(\boldsymbol{\sigma}, r, f, D) = \frac{J_2}{1-D} - \frac{1}{3}.\left[1 + q_3.f^2 - 2.q_1.f.\cosh\left(\frac{3.q_2.p}{2.\sigma_y}\right)\right].\sigma_y^2$$

(iv) Plastic flow and evolution equations for R, f and D

$$\dot{\boldsymbol{\varepsilon}}^{p} = \dot{\gamma}.\boldsymbol{N}$$

$$\dot{R} = -\dot{\gamma}.\frac{\partial \Phi}{\partial k}$$

$$\dot{f} = (1-g_0).\frac{f_N}{S_N\sqrt{2.\pi}}.\exp\left[-\frac{1}{2}\left(\frac{\bar{\varepsilon}^{p} - \varepsilon_N}{S_N}\right)^2\right].\dot{\bar{\varepsilon}}^{p} + (1-f).\dot{\varepsilon}_v^{p}$$

$$\dot{D} = g_0.\frac{D_N}{s'_N.\sqrt{2\pi}}.\exp\left[-\frac{1}{2}\left(\frac{\bar{\varepsilon}^{p} - \varepsilon'_N}{s'_N}\right)^2\right].\dot{\bar{\varepsilon}}^{p} + q_6.\dot{D}^{shear}.[g_0(\xi)]^{1/\|\eta\|+k}$$

where,

$$\dot{D}^{shear} = q_3 D^{q_4}\bar{\varepsilon}^{p}.\dot{\bar{\varepsilon}}^{p}$$

$$g_0 = 1 - |\bar{\theta}|$$

and,

$$\dot{\bar{\varepsilon}}^{p} = \sqrt{\frac{2}{3}(\dot{\boldsymbol{\varepsilon}}^{p} : \dot{\boldsymbol{\varepsilon}}^{p})} \qquad \dot{\varepsilon}_v^{p} = \mathrm{tr}(\dot{\boldsymbol{\varepsilon}}^{p})$$

(v) Loading/unloading criterion

$$\dot{\gamma} \geq 0, \qquad \Phi \leq 0, \qquad \dot{\gamma}\Phi = 0$$

3 NUMERICAL INTEGRATION ALGORITHM

Algorithms based on operator split methodology are especially suitable for the numerical integration of the evolution problem and have been widely used in computational plasticity (see Simo & Hughes [25]; De Souza Neto et al. [8]). This method, which is used for our development, consists of splitting the problem in two parts: an elastic predictor, where the problem is assumed to be elastic and, a plastic corrector, in which the system of residual equations comprising the elasticity law, plastic consistency and the rate equations is solved, taking the results of the elastic predictor stage as initial conditions. In the case of the yield condition has been violated, the plastic corrector stage is initiated and the Newton- Raphson

procedure is used to solve the discretised equations. The Newton-Raphson procedure was chosen motivated by the quadratic rates of convergence achieved which results in return mapping procedures computationally efficient, see Simo & Hughes [25] and De Souza Neto et al. [8]. The implicit algorithms were proposed initially based on the infinitesimal strain theory and here, both numerical models are extended to the finite strain through the framework based on a logarithmic strain measure, rather than the elastic deformation gradient, see Peric´ et al. [18] and Eterovic et al. [10]). The overall algorithm for numerical integration is summarized in Box 2.

Box 2. Fully implicit Elastic predictor/Return mapping algorithm.

(i) Evaluate elastic trial state: Given the incremental strain $\Delta\boldsymbol{\varepsilon}$ and the state variables at t_n:

$$\begin{array}{lll} \boldsymbol{\varepsilon}^{e\,trial}_{n+1} = \boldsymbol{\varepsilon}^{e}_{n} + \Delta\boldsymbol{\varepsilon} & ; & \bar{\varepsilon}^{p\,trial}_{n+1} = \bar{\varepsilon}^{p}_{n} \quad ; \quad R^{trial}_{n+1} = R_n \\ f^{trial}_{n+1} = f_n & ; & D^{trial}_{n+1} = D_n \quad ; \quad \boldsymbol{S}^{trial}_{n+1} = 2G\boldsymbol{\varepsilon}^{e\,trial}_{n+1} \\ p^{trial}_{n+1} = K\varepsilon^{e\,trial}_{v\,n+1} & ; & \sigma^{trial}_{y} = \sigma_y\left(R^{trial}_{n+1}\right) \end{array}$$

(ii) Check plastic admissibility:

IF $\Phi^{trial} = \frac{J_2^{trial}}{1-D^{trial}_{n+1}} - \frac{1}{3}.\left[1 + q_3.f^{trial\,2}_{n+1} - 2.q_1.f^{trial}_{n+1}.\cosh\left(\frac{3.q_2.p^{trial}_{n+1}}{2.\sigma^{trial}_{y}}\right)\right].\left(\sigma^{trial}_{y}\right)^2 \leq 0$

THEN set $(\cdot)_{n+1} = (\cdot)^{trial}_{n+1}$ ***(elastic step)*** and go to *(v)*

ELSE go to (iii)

(iii) Return mapping ***(plastic step)***: *Solve the system of equations below for* $\Delta\gamma, p_{n+1}, f_{n+1}$, R_{n+1} and D_{n+1}, *using Newton-Raphson method:*

$$\left\{\begin{array}{c} \dfrac{J_{2\,n+1}^{trial}}{\left[1+\left(\frac{2G.\Delta\gamma}{1-D_{n+1}}\right)\right]^2.(1-D_{n+1})} - \dfrac{1}{3}.\left[1 + q_3.{f_{n+1}}^2 - 2.q_1.f_{n+1}.\cosh\left(\dfrac{3.q_2.p_{n+1}}{2.\sigma_y}\right)\right].\sigma_y^2 \\ p_{n+1} - p^{trial}_{n+1} + \Delta\gamma.K.\sigma_y.q_1.q_2.f_{n+1}.\sinh\left(\dfrac{3.q_2.p_{n+1}}{2.\sigma_y}\right) \\ f_{n+1} - f^{trial}_{n+1} - \Delta f^{n} - \Delta f^{g} \\ R_{n+1} - R^{trial}_{n+1} - \Delta R \\ D_{n+1} - D^{trial}_{n+1} - \Delta D^{n} - q_6.\Delta D^{shear} \end{array}\right\} = \left\{\begin{array}{c} 0 \\ 0 \\ 0 \\ 0 \\ 0 \end{array}\right\}$$

where,

$$\Delta f^{n} = (1 - g_{0\,n+1}).\frac{f_N}{S_N\sqrt{2.\pi}}.\exp\left[-\frac{1}{2}\left(\frac{\bar{\varepsilon}^{p}_{n+1} - \varepsilon_N}{S_N}\right)^2\right].\Delta\bar{\varepsilon}^{p}$$

$$\Delta f^{g} = (1 - f_{n+1}).\Delta\gamma.\sigma_y.q_1.q_2.f_{n+1}.\sinh\left(\frac{3.q_2.p_{n+1}}{2.\sigma_y}\right)$$

continue Box 2.

$$\Delta R = \frac{\Delta\gamma}{(1-f_{n+1}-D_{n+1})}.\left\{q_1.q_2.f_{n+1}.p_{n+1}.\sinh\left(\frac{3.q_2.p_{n+1}}{2.\sigma_y}\right) + \frac{2}{3}.\sigma_y.\left[1+q_3.{f_{n+1}}^2-2.q_1.f_{n+1}.\cosh\left(\frac{3.q_2.p_{n+1}}{2.\sigma_y}\right)\right]\right\}$$

$$\Delta D^n = g_{0\,n+1}.\frac{D_N}{S'_N\sqrt{2.\pi}}.\exp\left[-\frac{1}{2}\left(\frac{\bar{\varepsilon}^p_{n+1}-\varepsilon'_N}{S'_N}\right)^2\right].\Delta\bar{\varepsilon}^p$$

$$\Delta D^{shear} = [g_0]^{(1/\|\eta\|+k)}.q_4 D^{q_5}.\bar{\varepsilon}^p.\Delta\bar{\varepsilon}^p \qquad g_0 = (1-\xi^2_{n+1})$$

(iv) Update the others state variables:

$$\boldsymbol{\varepsilon}^e_{n+1} = \boldsymbol{\varepsilon}^{e\,trial}_{n+1} - \Delta\gamma.\left[\frac{\boldsymbol{S}^{trial}_{n+1}}{\left[1+\left(\frac{2G.\Delta\gamma}{1-D_{n+1}}\right)\right].(1-D_{n+1})} + \frac{1}{3}.\sigma_y.q_1.q_2.f_{n+1}.\sinh\left(\frac{3.q_2.p_{n+1}}{2.\sigma_y}\right).\boldsymbol{I}\right]$$

(v) Exit

4 CALIBRATION PROCEDURE

In order to determine the materials parameters for the proposed constitutive model, two calibration points are required. The first point is taken from a specimen at high level of stress triaxiality, where a smooth bar specimen can be used. In this step, the hardening law, $\sigma_y(R)$, for the undamaged model is determined as well as the set of parameters for nucleation of micro void mechanism $[f_N, S_N, \varepsilon_N]$. The second calibration point can be taken from a specimen in pure shear loading condition, where the accelerator parameter, q_6, is determined as well as the set of parameters for the nucleation of micro defects mechanism $[D_N, S'_N, \varepsilon'_N]$. Here, a butterfly specimen can be used under pure shear loading condition.

4.1 Geometry and mesh definition

Regarding the material properties for the first calibration point, a classical smooth bar specimen is used and the following dimensions were employed (see Figure 2a). In order to trigger necking, a dimensional reduction of 5% in the central diameter of the specimen is used. For a steel 1045, a gauge section 20.6 mm is used. The standard eight-nodded axsymmetric quadrilateral element, with four Gauss integration points, is adopted. The initial mesh discretisation is illustrated in Figure 2b, where only one symmetric quarter of the problem, with the appropriate symmetric boundary conditions imposed to the relevant edges, is modeled. A total number of 1800 elements have been used in the discretisation of both the smooth specimens, amounting to a total of 5581 nodes.

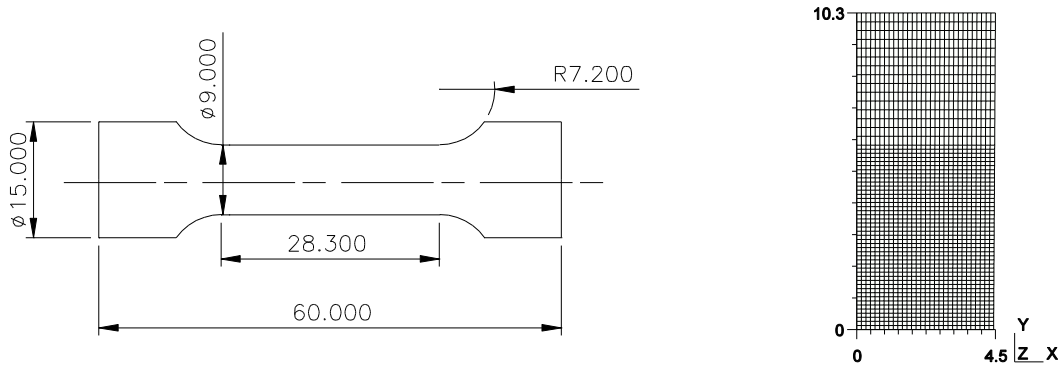

(a) (b)

Figure 2. Geometry for the smooth bar specimen. Dimension in (mm). Taken from Teng [26].

For the second calibration point and the numerical tests that will be presented, a butterfly specimen is used. The specimen was initially designed by Bai [2] and the geometry and general dimensions can be verified by Figure 3. In this case, a three dimensional finite element mesh of 3392 twenty nodded elements, with nine Gauss integration points, is used amounting to 17465 nodes.

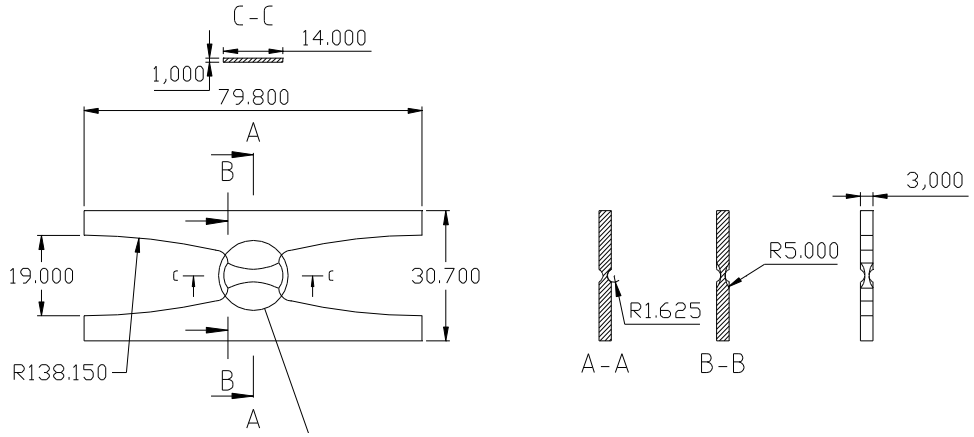

Figure 3. The geometry for butterfly specimen. Dimension in (mm). Taken from Bai [2].

4.2 Material parameters

In the present section, the stress-strain curve, the parameters required for modeling micro void nucleation mechanism from the GTN model are calibrated by tensile tests in cylindrical smooth bars. Through experimental data (see Bai [2]), the reaction versus displacement curve is determined as well as the stress-strain curve for an elasto-plastic model of von Mises type. The inverse method is adopted in order to calibrate the material parameters for coupled damage model by forcing the numerical solution to be, as close as possible to the experimental results. Figure 4a shows reaction curve for the model determined after the application of inverse method. A good agreement between the experimental and numerical results can be observed. Furthermore, the critical volume void fraction is also determined in the point where the model attains the displacement to fracture, experimentally observed (see Figure 4b). The critical values obtained is $f_c = 0.076$, for aluminum a steel 1045.

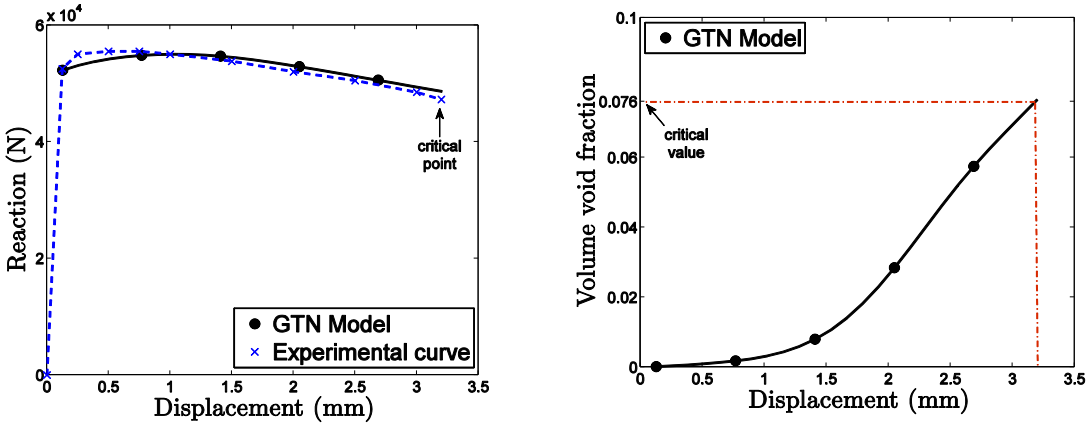

(a) (b)

Figure 4. (a) Reaction versus displacement curve for GTN model and experimental results for steel 1045. (b) Critical volume void fraction parameter calibrated for the material.

The results of the calibration procedure, in terms of stress-strain curve, can also be observed in Figure 5, where for uncoupled and coupled damage models, were determined.

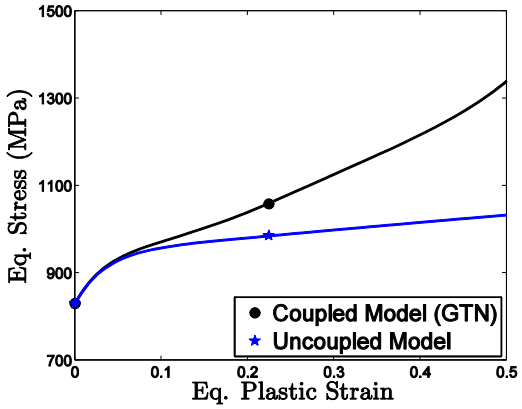

Figure 5. Stress-strain curve determined for an uncoupled and coupled models.

Regarding the second calibration point, the parameters related with the micro defects nucleation mechanism are determined as well as the critical value for the shear damage. The butterfly specimen is here used under pure shear loading condition and the displacement at fracture was suggested by Bai [2]. An inverse method is also adopted, regarding the calibration of the parameters by forcing the numerical results to be as close as possible to the experimental data. Table 2 contents the best materials parameters suggested after some inverse numerical tests. The parameters will be used during all numerical simulations.

Table 1: Materials parameters for steel 1045.

High stress triaxiality	f_N	S_N	ε_N	q_1	q_2	q_3	f_c	E (MPa)	υ
	0.05	0.2	0.1	1.5	1.0	2.25	0.076	220.000	0.33
Low stress triaxiality	d_N	S_N	ε_N	q_6		k	D_c		
	0.10	0.15	0.10	1.00		0.10	0.16		

5 NUMERICAL RESULTS

Regarding a consistent analysis for the new constitutive formulation at low level of stress triaxiality, some numerical tests are performed using the butterfly specimen and the implicit algorithm developed in above sections. Three different loading conditions are taken as: pure shear (0º), shear/tensile (10º) and shear/compression (-5º), taken hand the materials properties for a steel 1045. The performance of some internal variable and the ability to predict the correct fracture location are evaluated. At the end, the numerical results determined by the new formulation can be compared with the results obtained by other shear mechanisms as Xue [28] and Nahshon & Hutchinson [17].

Table 2: Numerical results for butterfly specimen, regarding different loading conditions.

Angle	Experimental data		Numerical results			
	u_f	$\bar{\varepsilon}^p$	u_f	$\bar{\varepsilon}^p$	f	d
0º	1.03	0.50	1.03	0.522	0.000	0.160
10º	0.42	0.36	0.44	0.353	0.026	0.053
-5º	1.71	0.60	1.71	0.612	0.000	0.126

Figure 6 represents a comparative illustration for the ability to predict the fracture location in combined shear/tensile (10º) loading condition using 1045 steel, regarding different shear mechanisms. Figure 6a illustrate the contour of damage parameter for Nahshon & Hutchinson shear mechanism, Figure 6b for Xue shear mechanism and Figure 6c for the new proposition. We can observer that only the new proposition predicts fracture onset in agreement with experimental evidence. The prediction by Xue is in complete disagreement with experimental evidence and by Nahshon & Hutchison, the contour is somewhat spread around the critical section, which may suggest a certain vagueness to the model.

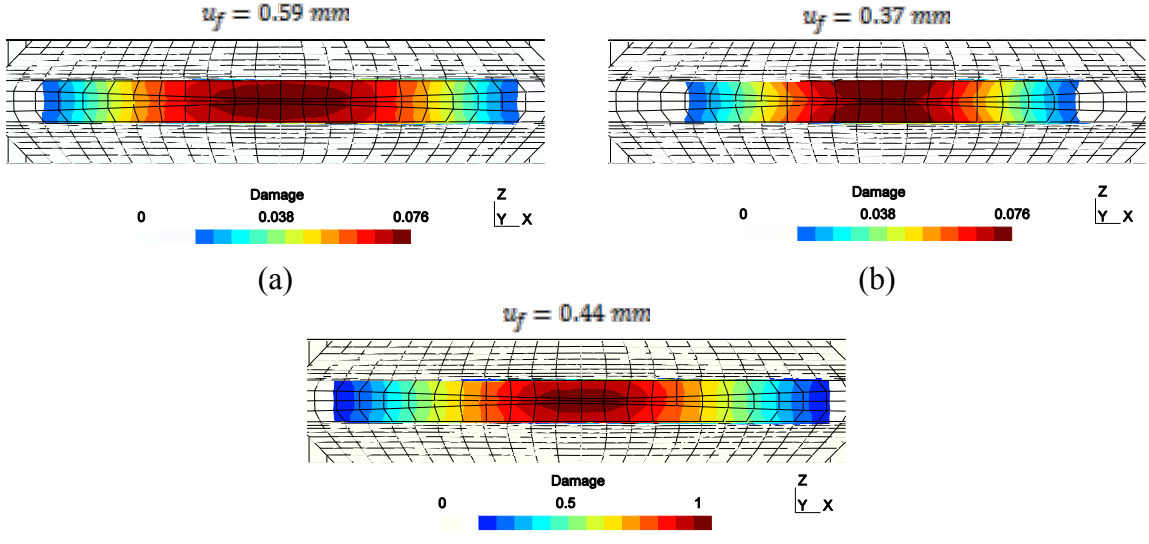

Figure 6. Damage parameter contour, (a) Nahshon & Hutchinson shear mechanism, (b) Xue shear mechanism and (c) new proposition. Section CC in the critical zone.

6 CONCLUSIONS

In this contribution, it was proposed a new formulation for improve the original GTN model, regarding the ability to predict ductile fracture in low level of stress triaxialities. The new formulation has two damage parameters, first one affecting only the hydrostatic stress part and another affecting the deviatoric part.

Numerical tests were provided, based on implicit integration algorithm, in order to evaluate the formulation in prediction the crack formation. A butterfly specimen was required, besides to a steel 1045. The model behaves well, whether in the determination of the correct level of equivalent plastic strain and displacement at fracture, or in prediction of the location to crack formation.

The proposition of create two damage parameters affecting separated stress contribution brings a balance in the evolution of internal variables so the more precise values at time of crack formation. Furthermore, the creation of a new micro-defects nucleation mechanism allowed a better calibration model and thus a good performance within wide range of stress triaxialities.

REFERENCES

[1] Andrade Pires, F.M., César de Sá, J.M.A., Costa Sousa, L., Natal Jorge, R.M. (2003). Numerical Modeling of ductile plastic damage in bulk metal forming, *International Journal of Mechanical Sciences*, 45:273–294.

[2] Bai, Y. (2008). Effect of Loading History on Necking and Fracture. Ph.D Thesis, *Massachusetts Institute of Technology*.

[3] Besson, J., Steglich, D. and Brocks, W. (2001). Modeling of crack growth in round bars and plane strain specimens. *International Journal of Solids and Structures*, 38(46–47):8259–8284.

[4] Besson, J., (2010). Continuum Models of Ductile Fracture: A Review. *International Journal of Damage Mechanics*, 19:3-52.

[5] Butcher, C., Chen, Z., Bardelcik, A., Worswick M. (2009). Damage-based finite-element modeling of tube hydroforming. *International Journal of Fracture*, 155:55–65.

[6] Chaboche, J.L. (2003). Damage mechanics. *In: Milne, I., Ritchie, R.O. and B. Karihaloo (eds.) Comprehensive Structural Integrity*, vol. 2. Elsevier-Pergamon, pp. 213–284.

[7] Chaboche, J.L., Boudifa, M., Saanouni, K., (2006). A CDM approach of ductile damage with plastic compressibility. *International Journal of Fracture*, 137:51–75.

[8] De Souza Neto, E.A., Peri´c, Owen, D.R.J. (2008). Computational methods for plasticity: theory and applications. *John Wiley & Sons Ltd*.

[9] Engelen, Roy A.B. (2005). Plasticity-induced Damage in Metals / nonlocal modelling at finite strains. PhD Thesis – Eindhoven : Technische Universiteit Eindhoven.

[10] Eterovic, A.L., & Bathe, K.-J. 1990. A Hyperelastic Based Large Strain Elasto-Plastic Constitutive Formulation with Combined Isotropic-Kinematic Hardening Using the Logarithmic Stress and Strain Measures. Int. *J. Num. Meth. Engng.*, 30, 1099–1114.

[11] Gurson, A.L. (1977). Continuum Theory of ductile rupture by void nucleation and growth - Part I. Yield criteria and flow rules for porous ductile media. *J. Engrg. Mat. Tech.,* 99:2-15.

[12] Lemaitre, J. (1985). A continuous damage mechanics model for ductile fracture. *Journal of Engineering Materials and Technology - Trans. of the ASME*, 107:83–89.
[13] Lemaitre, J., Chaboche, J.L. (1990). Mechanics of Solid Materials. Cambridge Univ. Press.
[14] Malcher, L.; Andrade Pires, F.M.; César de Sá, J.M.A. (2011). An Assessment of Isotropic Damage Constitutive Models under High and Low Stress Triaxialities. *International Journal of Plasticity*.
[15] McClintock, F. A. (1968). A Criterion for Ductile Fracture by the Growth of Holes. J. Appl. Mech., 35, 363–371.
[16] Mudry, F. (1985). Methodology and application of local criteria for prediction of ductile tearing. D.Reidel Publishing Co.
[17] Nahshon, K., Hutchinson, J. (2008). Modification of the Gurson model for shear failure. *European Journal of Mechanics A/Solids,* 27:1–17.
[18] Peric, D., Owen, D.R.J., & Honnor, M.E. (1992). A Model for Finite Strain Elasto-Plasticity Based on Logarithmic Strains: *Computational Issues. Comp. Meth. Appl. Mech Engng.*, 94:35–61.
[19] Pineau, A. (1981). Review of fracture mechanisms and local approaches to predicting crack resistance in low strength steels. In: Franc¸ois, D. et al. (ed.) Advances in Fracture Researches. New-York, Pergamon Press, ICF5. Cannes.
[20] Reis, F.J.P.; Malcher, L. ; Andrade Pires, F.M. ; César de Sá, J.M.A. (2010). A modified GTN model for the prediction of ductile fracture at low stress triaxialities. *International Journal of Structural Integrity*.
[21] Rice, J. R., Tracey, D., M. (1969). On the ductile enlargement of voids in triaxial stress fields. *Journal of the Mechanics and Physics of Solids*, 17:201–217.
[22] Rousselier's, G. (1980). Finite deformation constitutive relations including ductile fracture damage. In: Nemat-Nasser (ed.) Three-Dimensional Constitutive Relations and Ductile Fracture. North-Holland Publ. Comp., 1981 pp. 331–355.
[23] Rousselier's, G. (1987). Ductile fracture models and their potential in local approach of fracture. *Nuclear Engineering and Design* 105: 97–111.
[24] Rousselier's, G. (2001). The Rousselier model for porous metal plasticity and ductile fracture. In: Lemaitre, J. (ed.) Handbook of Materials Behavior Models, vol. 2. Academic Press, New York, chapter 6.6, pp. 436–445.
[25] Simo, J.C., & Hughes, T.J.R. (1998). Computational Inelasticity. NY: Springer-Verlag.
[26] Teng, X. (2008). Numerical prediction of slant fracture with continuum damage mechanics. *Engineering Fracture Mechanics*, 75:2020–2041.
[27] Tvergaard, V. and Needleman, A. (1984). Analysis of the cup-cone fracture in a round tensile bar. *Acta Met.* 32:157–169.
[28] Xue, L. (2007). Ductile Fracture Modeling – Theory, Experimental Investigation and Numerical Verification, Ph.D Thesis, *Massachusetts Inst. of Technology*. Ph.D Thesis, *Massachusetts Inst. of Technology*.